Final Report on the Eye Problem
Maths in Medicine Study Group, Nottingham 2006

January 29, 2007

Contents

1 Summary of the problem presented

Unless otherwise referenced, the information in this section was obtained from the presenter Alex Foss during the study group. Further details can be found in the relevant experimental literature (for example, [1]).

1.1 Glaucoma and papilloedema

The retinal ganglia are neurons which relay visual signals from the eye to the brain. Each ganglion consists of a dendritic cellular body in the retina (on the inside of the eye) and a long axon which goes from the retina, passes through the back of the eye and ultimately reaches the lateral geniculate nucleus in the brain. Between the eye and the brain the axons of the retinal ganglia are bundled together to form the optic nerve.

Various medical conditions are known to affect vision by causing the death of some of the retinal ganglia. Two such conditions are glaucoma and papilloedema, which are both characterised by an imbalance in hydrostatic pressure between the eye and the brain. The fluid of the eye (the aqueous) and the fluid that surrounds the brain and spinal chord (the cerebrospinal fluid or CSF) are both maintained under pressure by separate mechanisms. In healthy people these two pressures are almost the same, but in glaucoma the pressure in the eye, the intraocular pressure, is elevated (with no change in the CSF pressure) and in papilloedema the pressure in the CSF near the eye is elevated (with no change in the intraocular pressure). However, in both cases similar patterns of ganglion death leading to loss of vision are observed.

As the axons of the retinal ganglia exit the eye they pass through the firm outer layer of the eye called the sclera. The axons exit through a perforated region of the sclera called the lamina cribrosa, literally the 'sieve-like layer'. This is shown in Figure 1. Each perforation of the lamina cribrosa admits the passage of several hundred axons but the perforations are not large enough to allow fluid to pass freely between the eye and the surrounding tissue. This means that a pressure difference between the eye and the CSF cannot be relieved by a flow of fluid across the lamina cribrosa. The lamina cribrosa is mechanically weaker than the sclera and in severe cases of glaucoma or papilloedema it deforms to accommodate the pressure difference. In severe glaucoma the lamina cribrosa is observed to bend backwards out of the eye, while in severe papilloedema it bends into the eye.

A further complexity is that the retinal ganglia do not die uniformly across the optic nerve. Instead, cells in the twelve o'clock and six o'clock positions are found to die first and peripheral vision (corresponding to the axons on the perimeter of the optic nerve) is affected before central vision. Another feature of these conditions is that glaucoma and papilloedema are

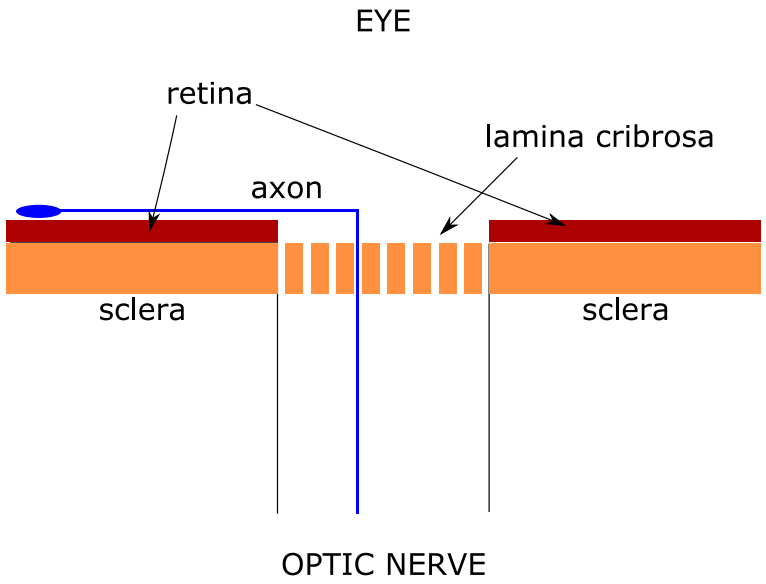

Figure 1: Diagram showing a retinal ganglion cell (blue) as its axon passes out of the eye and into the optic nerve. Note that the axon must make a sharp turn to pass through the lamina cribrosa. Diagram is illustrative only and is not to scale.

both gradual conditions in which the ganglia die over a period of years.

When ganglia die as a result of glaucoma or papilloedema it is observed that the region of the axon outside the eye dies before the region of the rest of the cell inside the eye. The dominant theory as to why ganglia die in this manner is that the axons of the cells are pinched by the deforming lamina cribrosa in a process called defenestration. This leads to a physical obstruction that prevents proteins produced in the main body of the cell (*i.e.* in the eye) from reaching any part of the cell beyond the lamina cribrosa. However, in contradiction to this theory it is found that significant nerve death occurs before any noticeable deformation in the lamina cribrosa.

Another possible mechanism of cell death involves rupture of the axons at the point where they bend from going along the retina to going through the lamina cribrosa (shown in Figure 1). This bend is close to a right angle, and might lead to a weak point on the axon that could be damaged by stresses arising from high pressure differences.

In order to understand which mechanism of cell death actually occurs we investigated models of the ganglial axon as a long, thin tube passing between two regions held at different pressures. We used shell theory to describe the deformations of the membrane surrounding the axon, expecting to find a region in which the axon swelled beyond some limit that could lead to rupture. However, by treating the axonal membrane as being semi-permeable we found that the internal flow in the axon in response to the nonuniform external pressure

would be sufficient to completely disrupt the normal axoplasmic flow. This gives a novel and plausible explanation as to how ganglial death takes place even before deformation of the lamina cribrosa is observed.

1.2 Details of a single axon

Since glaucoma and papilloedema lead to the destruction of the optic nerve by causing the deaths of the axons of individual ganglia we found it appropriate to construct a mathematical model of the response of a single ganglial axon to the nonuniform external pressure applied along its length. Each axon has a radius of around 0.25 μm but a length of around 7 cm, so they may be thought of as very long and thin cylinders. It should be noted that axons are not straight; they bend at a right angle as they go from running along the surface of the retina to joining the optic nerve and they also take a highly tortuous route through the lamina cribrosa. However, the radius of curvature in these cases would appear to be always much larger than the radius of an individual axon, so for a first model it is appropriate to treat the axon as having cylindrical symmetry.

The lamina cribrosa has a width of around 0.2 mm and we would not expect the length of the axon in the lamina cribrosa to be any longer than a millimetre despite the tortuous path that it takes through this region. This is very short compared to the total length of the axon, so we can ignore the segment of the axon that passes through the lamina cribrosa and treat the transition from the eye to the optic nerve as an abrupt change in the external pressure experienced by the axon. However, we ultimately find that the length-scale over which significant variation in pressure occurs is comparable to the length of the axon in the lamina cribrosa and so it may be necessary to reexamine the validity of this assumption.

The axon is bounded by a membrane along its length. This membrane consists of a simple lipid bilayer for the section of the axon in the eye and for a short distance into the optic nerve, but it is myelinated for most of the optic nerve. Over a short time scale the membrane is basically inextensible, but an axon can adapt its membrane if it is under pressure to widen or thin. The myelinated part of the axon is stiffer than a simple lipid bilayer, but should behave in largely the same way. In our mathematical model, the membrane is treated as if it had the same physical properties along the full length of the axon.

One important feature of the axon membrane is that it is permeable to water and small solutes. However, the axoplasm (fluid inside the axon) has a different composition to the fluid outside the axon. This is partly because the cell contains large proteins that cannot pass through the membrane wall and partly because of ion channels that regulate the sodium and potassium contents of the axon. The fact that there is more dissolved material inside the axon than outside it leads to an osmotic pressure difference across the cell membrane. If the combined osmotic and hydrostatic pressures on each side of the membrane do not

balance, there will be a flow of water into or out of the axon. This is an important part of our model, as it describes a way in which the axon accommodates the pressure differences it experiences.

There exist some published experimental data on the permeability of the axon membrane [2, 3]. However, each of these papers gives significantly different values for permeability inferred from experiments involving an imposed osmotic pressure difference compared to experiments involving an imposed hydrostatic pressure difference. We could find no physical reason why these permeabilities should be different, let alone different by three orders of magnitude as in these papers. Hence, while we use the experimental values for permeability in determining the parameters of our model it would seem likely that the published data is unreliable.

Far into the eye, the pressure in an axon is in equilibrium with the intraocular pressure; far into the brain, it is in equilibrium with the CSF pressure. If these are different, the fact that there is a pressure difference along the length of the axon will result in a flow down the axon from the high pressure region to the low pressure region. We choose to describe the relationship between flow along the axon and pressure changes using Poiseuille's law rather than other possibilities such as Darcy's law. This is because the flow is very slow and hence laminar. However it is not immediaely obvious what obstacles will create the main viscous resistance to the flow. We use Poiseuille flow here, where the main resistance is due to the walls of the axon, as our model will require us to characterise how the resistance changes with deformation of the axon and in this case this is relatively easy while Darcy's law would require more details to be considered. In keeping with this simple model of the flow we shall assume that any imbalance between the fluid forces internal and external to the axon will be counteracted by forces due to deformation of the axon. Following our simplification for the flow behaviour, these forces will be assumed to be generated by the outer wall of the axon rather than any internal structure.

2 Development of mathematical model

As discussed in Section 1.2, a single ganglial axon can be considered as a long, thin, cylindrical tube that passes between two regions held at different pressures. The axon adapts to this pressure difference in a number of ways. Firstly, and most importantly, the axon is permeable to water and so unless the hydrostatic pressure difference is balanced by an osmotic pressure difference water will flow into the axon on the high-pressure side and out again on the low-pressure side. Also, the axon radius can change to accommodate the difference between the hydrostatic pressures on either side of the axon membrane.

Our mathematical model seeks to describe how the rate of flow in the axoplasm, the internal pressure profile and the axon radius vary along the length of the axon if we specify the external hydrostatic pressures along the axon and the mechanical properties of the axonal membrane. In order to model the pressure and flow in the axon, we use the theory of fluid flow in a narrow pipe, obtaining the results given in Section 2.1. To describe the deformation of the axon due to the balance of external and internal pressures, we use shell-theory, obtaining the results given in Section 2.2. This gives us a six-equation model that is quite complicated, so we simplify the system by nondimensionalising and determining which terms are significant to leading order, obtaining the results given in Section 2.3. The final model is summarised in Section 2.4.

Further mathematical details for these sections are given in Appendices A to C respectively.

2.1 Flow along and through an axon

This section may be considered to be a summary of Appendix A. For more details of any of the steps described here, see Appendix A.

Consider a long, thin, cylindrical tube containing a laminar fluid flow with a low Reynolds number. Fluid flow is described by the Navier-Stokes equations, which simplify in this situation to the following:

$$\begin{aligned} \frac{\partial u}{\partial z} + \frac{1}{r}\frac{\partial}{\partial r}(rv) &= 0, \\ \frac{\partial P}{\partial r} &= 0, \\ -\frac{\partial P}{\partial z} + \frac{\mu}{r}\frac{\partial}{\partial r}\left(r\frac{\partial u}{\partial r}\right) &= 0, \end{aligned} \tag{1}$$

where z and r are the first and second cylindrical coordinates, $u(z,r)$ is fluid velocity in the z direction, $v(z,r)$ is fluid velocity in the r direction, $P(z,r)$ is the pressure of the fluid inside

the tube and μ is the coefficient of dynamic viscosity (equal to 8.9×10^{-4} Pa s for water).

Using the mathematical analysis given in Appendix A, we find that the fluid velocity in the z direction at any point in the cylinder is given by

$$u(z, r) = \frac{r^2 - R^2}{4\mu} \frac{dP}{dz},$$

where R is the radius of the cylinder at any point. It should be noted that R must vary slowly with z in order for the assumptions underlying this working to be valid. We can integrate this equation across a perpendicular cross-section of the axon to find the total flux of axomplasm along the tube as a function of z. This gives

$$F(z) = -\frac{\pi R^4}{8\mu} \frac{dP}{dz}. \tag{2}$$

This equation is known as Poiseuille's law.

Given our expression for $u(z, r)$, we can integrate equation (1) to find an expression for $v(z, r)$, the perpendicular fluid velocity. As the axon is permeable to water we expect v on the membrane to be determined by the flow across the permeable membrane that surrounds the axon. If κ is the permeability of the axon expressed as a velocity per unit of pressure difference and Δp is the difference in pressure across the boundary (including osmotic and hydrostatic pressures), we expect that

$$\kappa \Delta p = -v(z, R).$$

Hence, using the expression for $v(z, R)$ obtained in Appendix A, we find that

$$\kappa \Delta p = -\frac{1}{R} \frac{d}{dz} \left(\frac{R^4}{16\mu} \frac{dP}{dz} \right).$$

Now, Δp must include a contribution from osmotic pressure as well as from hydrostatic pressure. For simplicity, we assume that the concentration of the dissolved material, which leads to the osmotic pressure difference, is a constant along the length of the axon. The difference between the activity of this material and the dissolved material in the surrounding space gives us a constant osmotic pressure difference of Π everywhere on the axon, pulling fluid into the axon space. We now let P be the pressure inside the axon as before, but also introduce P_{ext} as the specified external pressure acting on the axon. This allows us to rewrite the above equation as

$$\kappa(P_{\text{ext}} + \Pi - P) = -\frac{1}{R} \frac{d}{dz} \left(\frac{R^4}{16\mu} \frac{dP}{dz} \right) \tag{3}$$

It should be noted that this equation may be thought of as a mass conservation equation for the fluid in the axon.

As mentioned before, experimental values of the permeability, κ, are rather unreliable as is indicated by the fact that they are given separately for hydrostatic and osmotic pressures in the biological literature [2, 3]. In SI units, the values found are of the order of 10^{-11} m s^{-1} Pa^{-1} for hydrostatic pressure and 10^{-14} m s^{-1} Pa^{-1} for osmotic pressure. Pragmatically, we will use the hydrostatic value of $\kappa = 10^{-11}$ m s^{-1} Pa^{-1} as, at least initially, we are concerned with a flow that is induced from hydrostatic pressure differences.

As a final note, we observe that equation (3) contains the definition of flux given in equation (2) and could also be written in the form

$$\kappa(P_{\text{ext}} + \Pi - P) = \frac{1}{2\pi R}\,\frac{dF}{dz}.$$

This is the equation that we would obtain if we considered sources and losses of water over a short length of the axon.

2.2 Membrane mechanics

In order to solve equation (3) we need to specify a relationship between the radius of the axon and the hydrostatic pressure difference across the axon wall. Most simply, we could say that the radius of the axon is some fixed constant along its entire length. However, in severe cases of glaucoma and papilloedema we expect that the change in pressure between the eye and the optic nerve could cause significant deformation of the axon wall. In order to deal with this appropriately, we wish to develop a more rigorous approach to the mechanics of membrane deformation. Even so, we found that even when mechanics were included (as described in Section 3.3) the flow of water through the axon was not substatially different to the constant radius work described in Section 3.1.

Interestingly, our work at the Study Group started from the premise that it is the mechanical deformation of the axon that is most important. We initially constructed equations to describe the equilibrium deformation of the axon and only later coupled these with the flow equations derived in Section 2.1. Flow was introduced in order to describe how the external pressure affected the pressures inside the axon, but ended up becoming the most important part of the model.

This section will describe (with additional details given in Appendix B) the work carried out using shell theory to obtain an expression for the radius of the axon in terms of the hydrostatic pressure difference, the tension along the body of the axon and the shear forces induced by flow through the axon.

In addition to internal stresses there are two external forces acting on our membrane. Firstly, there may exist a difference in pressures between the fluid on the inside of the axon (at a

pressure of P) and the fluid surrounding the axon (at a pressure of P_{ext}). This gives rise to a normal force per unit area on the axon membrane of $P - P_{\text{ext}}$. Note that as we are only considering hydrostatic forces in this case it is not necessary to include the osmotic pressure Π. Secondly, the flow along the axon induces shear forces on the wall of the axon that are proportional to the rate of flow. This appears as a term in the azimuthal force balance equation of $\frac{GR^2}{2}$, where G is the shear rate given by $G = -\frac{dP}{dz}$.

Thin structures such as membranes may be described using shell theory (see, for example, [4]). In this theory, the stresses within the membrane are represented by *so-called* stress resultants, which are effectively the averaged stresses across the thickness of the structure. This allows us to reduce our three dimensional problem to a two dimensional problem. In our case, we use stress resultants to describe three different sorts of internal 'forces' - tensions (represented by T), the normal stress resultants from shear in the membrane (represented by Q), and bending moments (represented by M). These are illustrated in Figure 2.

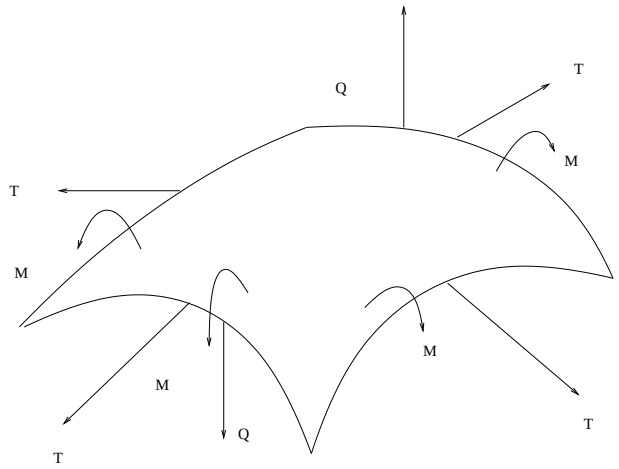

Figure 2: The tension T, bending moment M and normal shear resultant Q acting on a small element of the axon membrane. Together with the influence of the hydrostatic pressure difference across the membrane and the shear forces due to fluid flow along the axon, these forces define the shape that the membrane takes.

It should be noted that despite what is shown in Figure 2, T and M are not necessarily isotropic; this depends on the constitutive assumptions that are made. As described in Appendix B, the constitutive equations that we develop for the inextensible lipid bilayer of the axon membrane do in fact result in T and M both being isotropic, so Figure 2 is accurate for our specific case.

In addition to the variables already described, we will need ϕ, the angle formed between the tangent along the axonal membrane and a radius, and s, an arclength parameter. From the geometry of the system (pictured in Figure 5 in Appendix B) we find that ϕ can be defined

in terms of the changing radius as follows:

$$\frac{dR}{ds} = \cos\phi. \tag{4}$$

The arclength parameter s is defined so that the direction of s increasing is the direction of z decreasing. This is done because we are copying earlier work that was originally developed to model red blood cells, and the geometry of their problem made this the simplest approach. The relationship between s and z is given by

$$dz = -\sin\phi\, ds.$$

Following Pamplona and Calladine [5] (see [6] for a clear exposition) and applying our constitutive assumptions we ultimately derive the following system of four equations:

Axial force balance:

$$\frac{d}{ds}(RT) - T\cos\phi - \frac{d\phi}{ds}RQ = \frac{GR^2}{2},$$

Normal force balance:

$$\frac{d}{ds}(RQ) + \sin\phi T + RT\frac{d\phi}{ds} = (P - P_{\text{ext}})R,$$

Moment balance:

$$\frac{d}{ds}(MR) - M\cos\phi + RQ = 0,$$

Moment constitutive law:

$$M = B\left(\frac{d\phi}{ds} + \frac{\sin\phi}{R}\right);$$

where B is a constant of proportionality relating the moment to the total curvature.

In addition to these four equations, we have a definition of ϕ from (4)

$$\frac{dR}{ds} = \cos\phi,$$

and the fluid flow equation (3) from Section 2.1, thus giving us six equations in six unknowns (R, ϕ, T, Q, M and P).

We now apply a change of independent variable to rewrite all of these equations in terms of $\bar{s}$, the arclength parameterisation that would be obtained if the axon were deformed from its current state (without stretching) to one of uniform radius $\bar{r}$. This means that $\bar{s}$ is effectively a measure of arclength along the unstressed axon that would result from having a constant

external pressure applied along its length (*i.e.* equal intraocular and CSF pressures). We use $\bar{s}$ in preference to s because the constitutive assumption for T is generally phrased in terms of $\bar{s}$. Hence, this system allows us to potentially change the constitutive assumption that we used for tension without completely rewriting the model.

Incompressibility of the membrane means that the surface area of an element ds remains unchanged under pressure-induced deformation. That is, we find that $2\pi R\ ds$ is equal to $2\pi\bar{r}\ d\bar{s}$, or more succinctly:

$$\frac{ds}{d\bar{s}} = \frac{\bar{r}}{R}.$$

This ultimately gives us the relation

$$\frac{d}{ds} \equiv \frac{R}{\bar{r}}\ \frac{d}{d\bar{s}}.$$

Applying these changes yields the full system of equations given below. Note that we must first rewrite the flow equation in terms of s using the fact that $dz = -\sin\phi\ ds$.

$$\frac{R}{\bar{r}}\ \frac{d}{d\bar{s}}(RT) - T\cos\phi - \frac{R^2Q}{\bar{r}}\ \frac{d\phi}{d\bar{s}} = \frac{GR^2}{2} = \frac{R^3}{2\bar{r}\sin\phi}\ \frac{dP}{d\bar{s}},$$

$$\frac{R}{\bar{r}}\ \frac{d}{d\bar{s}}(RQ) + T\sin\phi + \frac{R^2T}{\bar{r}}\ \frac{d\phi}{d\bar{s}} = (P - P_{\text{ext}})R,$$

$$\frac{R}{\bar{r}}\ \frac{d}{d\bar{s}}(RM) - M\cos\phi + RQ = 0,$$

$$M = B\left(\frac{R}{\bar{r}}\ \frac{d\phi}{d\bar{s}} + \frac{\sin\phi}{R}\right),$$

$$\frac{R}{\bar{r}}\ \frac{dR}{d\bar{s}} = \cos\phi,$$

$$\kappa(P_{\text{ext}} + \Pi - P) = -\frac{1}{16\mu\bar{r}^2\sin\phi}\ \frac{d}{d\bar{s}}\left(\frac{R^5}{\sin\phi}\ \frac{dP}{d\bar{s}}\right).$$

With appropriate boundary conditions it would be possible to solve this system of equations numerically (since we have six equations in six unknowns). However, it is more useful to nondimensionalise the system and see if it is possible to determine which terms may be effectively discarded without significantly altering the solution to our system.

2.3 Nondimensionalisation and boundary conditions

In order to simplify the system of equations further, we nondimensionalise and consider which terms are significant given that $\bar{r}$ (the characteristic radius of the axon) is much smaller than

L (the characteristic length of the axon) and that ϕ will always be close to $\frac{\pi}{2}$.

A summary of the nondimensionalisations is given as follows:

$$R = \bar{r}R^*, \qquad P = p_b + (p_e - p_b)P^*, \qquad T = \bar{r}(p_e - p_b)T^*,$$
$$Q = \bar{r}(p_e - p_b)Q^*, \qquad M = \bar{r}^2(p_e - p_b)M^*, \qquad \bar{s} = L\sigma.$$

First, consider the nondimensionalisation to be used for pressure. One way of scaling pressure is to use the difference between the hydrostatic pressures in the eye and in the CSF. Hence, P is scaled so that

$$P = p_b + (p_e - p_b)P^*,$$

where P^* is the nondimensional pressure and p_e and p_b are the hydrostatic pressures in the eye and CSF (brain) respectively. Similarly, we define P^*_{ext} to be the nondimensional external pressure given by

$$P_{\text{ext}} = p_b + (p_e - p_b)P^*_{\text{ext}}.$$

This means that $P^*_{\text{ext}} \to 0$ on the brain side of the lamina cribrosa and $P^*_{\text{ext}} \to 1$ on the eye side of the lamina cribrosa. If we define $\bar{s}$ so that $\bar{s} = 0$ at the lacrima cribrosa (treated as having negligible width) and that $\bar{s} < 0$ in the eye and $\bar{s} > 0$ in the optic nerve, we obtain the following definition for $P^*_{\text{ext}}(\bar{s})$:

$$P^*_{\text{ext}}(\bar{s}) = \begin{cases} 1, & s < 0; \\ 0, & s > 0. \end{cases}$$

This scaling is very good for P_{ext} but (as discussed in Appendix C) it can lead to problems as p_e approaches p_b. In this case, P^* goes to infinity while P remains well-behaved and bounded. There may be advantages in scaling P with Π instead of with $p_e - p_b$.

The natural scale for the radius is $\bar{r}$ (as used previously in the definition of $\bar{s}$). By combining this length scale with the pressure scale we can obtain appropriate scales for T, Q and M (stated above). The last parameter to nondimensionalise is $\bar{s}$, the arclength along the axon. We do not yet have a 'feel' for the length scale over which significant changes of our dependent parameters take place, so we scale $\bar{s}$ to some unknown arbitrary length which we shall define later. This gives us $\bar{s} = L\sigma$ where σ is our dimensionless arclength parameter. Significantly, we expect L to be much larger than $\bar{r}$ so that $\epsilon = \frac{\bar{r}}{L}$ is dimensionless and small.

Since $\phi \approx \frac{\pi}{2}$, we can include a simplification for ϕ in our nondimensionalisation. Let $\phi = \frac{\pi}{2} - \epsilon\hat{\phi}$, using the same definition of ϵ as before. Hence, $\sin\phi \approx 1$ and $\cos\phi \approx \epsilon\hat{\phi}$.

Applying the nondimensionalisations summarised above and rearranging so that ϵ and $\hat{\phi}$ are

included as appropriate, we obtain the following system of equations:

$$\begin{aligned}
\epsilon R^* \frac{d}{d\sigma}(R^* T^*) - \epsilon \hat{\phi} T^* + \epsilon^2 R^{*2} Q^* \frac{d\hat{\phi}}{d\sigma} &= \epsilon \frac{R^{*3}}{2} \frac{dP^*}{d\sigma}, \\
\epsilon R^* \frac{d}{d\sigma}(R^* Q^*) + T^* + \epsilon^2 R^{*2} T^* \frac{d\hat{\phi}}{d\sigma} &= (P^* - P^*_{\text{ext}}) R^*, \\
\epsilon R^* \frac{d}{d\sigma}(R^* M^*) - \epsilon \hat{\phi} M^* + R^* Q^* &= 0, \\
M^* &= \tilde{B} \left(\frac{1}{R^*} - \epsilon^2 R^* \frac{d\hat{\phi}}{d\sigma} \right), \\
\hat{\phi} &= R^* \frac{dR^*}{d\sigma}, \\
\alpha \frac{d}{d\sigma} \left(R^{*5} \frac{dP^*}{d\sigma} \right) + \left(P^*_{\text{ext}} + \tilde{\Pi} - P^* \right) &= 0;
\end{aligned}$$

where $\tilde{B}$, α and $\tilde{\Pi}$ are dimensionless constants given by

$$\tilde{B} = \frac{B}{\bar{r}^3 (p_e - p_b)}, \qquad \alpha = \frac{\bar{r}^3}{16 \mu \kappa L^2}, \qquad \tilde{\Pi} = \frac{\Pi}{p_e - p_b}.$$

The dimensionless parameter α may be thought of as defining the rate of flow along the axon relative to that through the wall, while $\tilde{B}$ is the nondimensional bending stiffness and $\tilde{\Pi}$ represents a nondimensional osmotic force. Large $\tilde{B}$ corresponds to the case where the bending moment around a section of the axon with radius $\bar{r}$ is significantly larger than $\bar{r}^2(p_e - p_b)$. It is not immediately obvious whether this is the case or not, particularly since $p_e - p_b$ goes to zero in models of a healthy eye. However, following the work done during the study group, we assume that the force across the membrane due to the pressure difference is not significantly smaller than the bending moment around the tube. The validity of this assumption would possibly be clearer if we adopted the different scaling for pressure discussed earlier. Using our assumption, we considered the distinguished limit where $\tilde{B} = O(1)$. The working for this is given in Appendix C.

Ultimately, we find that when $\tilde{B} = O(1)$ (or even $o(\epsilon^{-2})$) the variables Q and M decouple from the system to leading order. We can therefore discard them and consider a simplified system including only $\hat{\phi}$, R^*, T^* and P^*. This in turn can be simplified further by substituting T^* and $\hat{\phi}$ out of the equations using the fact that $\hat{\phi} = R^* \frac{dR^*}{d\sigma}$ as stated above and

$$T^* = R^*(P^* - P^*_{\text{ext}}) \tag{5}$$

based on the leading order expansion described in Appendix C. We are left with two equations

for the two unknowns R^* and P^* as follows:

$$\alpha \frac{d}{d\sigma}\left(R^{*5}\frac{dP^*}{d\sigma}\right) + \left(P^*_{\text{ext}} + \tilde{\Pi} - P^*\right) = 0, \tag{6}$$

$$\frac{d}{d\sigma}(R^*(P^* - P^*_{\text{ext}})) = \frac{R^*}{2}\,\frac{dP^*}{d\sigma}. \tag{7}$$

This system is an appropriate description of the deformations of our axon and pressure gradients along the axon for the case where $\tilde{B}$ is not large.

As a side issue, let us consider how flux (as defined in equation (2)) has been changed by the nondimensionalisation. In the original equation (dimensional) equation we find that

$$F(z) = -\frac{\pi R^4}{8\mu}\,\frac{dP}{dz}.$$

However, the corresponding term in equation (6) takes the form

$$F^*(\sigma) = R^{*5}\frac{dP^*}{d\sigma}. \tag{8}$$

¿From our earlier nondimensionalisation, we know that $R = \bar{r}R^*$, $P = p_e + (p_b - p_e)P^*$ and (from combining several steps)

$$dz = -\frac{L\sin\phi}{R^*}d\sigma \approx -\frac{L}{R^*}d\sigma.$$

Hence,

$$\begin{aligned} F &= -\frac{\pi R^4}{8\mu}\,\frac{dP}{dz} \\ &= \frac{\pi \bar{r}^4 R^{*5}}{8\mu}\,\frac{p_e - p_b}{L}\,\frac{dP*}{d\sigma} \\ &= \frac{\pi \bar{r}^4 (p_e - p_b)}{8\mu L}F^*. \end{aligned} \tag{9}$$

This gives us a way to convert the nondimensional results for flux that we will obtain into results that can be interpreted physically. Henceforth, stars will be omitted from dimensionless variables.

Now, the parameter α in equation (6) is particularly interesting as it gives us a way of determining the characteristic length scale over which the dependant variables of the problem change significantly. If we were to choose L to be the entire length of the axon (around 7 cm) and used experimental values of the other constants in the definition of α we would find that α is very small. This in turn leads to equation (7) displaying boundary layer properties;

significant changes in the dependent variables only occur within a region where σ is close to 0. Since the behaviour that we are concerned with is not significant throughout the axon, we can choose L to be some smaller value so that we 'focus in' on the important changes.

The most natural way to do this is to choose L so that $\alpha = 1$. That is,

$$L = \sqrt{\frac{\bar{r}^3}{16\mu\kappa}}.$$

This means that L will be characteristic of the width of the boundary layer rather than the length of the entire axon.

Expressing reported experimental results in SI units, we find that $\bar{r} = 2.5 \times 10^{-7}$ m, $\mu = 8.9 \times 10^{-4}$ Pa s and $\kappa \approx 10^{-11}$ m s^{-1} Pa^{-1}. Based on these numbers, we find that $L \approx 3 \times 10^{-4}$ m, which is much smaller than the length of the entire domain but not siginificantly larger than the width of the lamina cribrosa. This is not a problem in the case where we assume constant R because we can treat the tube passing through the lamina cribrosa as being surrounded by an impermeable layer, yielding the result that the flux of fluid is constant throughout the entire middle section. Even when we do not assume constant R we will not include the lamina cribrosa in this work because of the added complexity that it would involve. Hence, a possible extension to this model would be to consider in detail the behaviour of the axon as it passes through this region.

Boundary conditions

As described earlier, we take the lamina cribrosa to be an infinitesimally thin layer at $\sigma = 0$. Furthermore, we define the region where σ is negative to be the eye and the region where σ is positive to be the optic nerve/brain. Arbitrarily, we take the intraocular pressure to be greater than the hydrostatic pressure in the CSF (the case in glaucoma), but the symmetry of the problem means that the result for papilloedema would be the same only reveresed. Conveniently, when we consider the case of glaucoma, $p_e - p_b$ will be positive.

In the case where R varies along the length of the axon, we need a boundary condition on R. This can be obtained from the fact that the axon membrane is inextensible and the two ends of the axon are fixed; the dendritic cell body communicates with other cells in the retina and cannot move, and similarly the axon ends in a synapse in the brain that would not function properly if the axon end moves. This allows us to effectively construct a 'mass conservation' equation for the length of the axon.

Let L_e and L_b be the length of the axon in the eye and the brain respectively (both large numbers with our nondimensionalisation). Let s^* be the nondimensionalised form of the original untransformed arclength parameter (scaled against L). If the axon is of fixed length, then the integral of 1 with respect to s^* over the entire axon must be equal to $L_e + L_b$. That

is,

$$\int_{-L_e}^{L_b} ds^* = \int_{-L_e}^{L_b} \frac{1}{R} d\sigma = L_e + L_b.$$

If we take it that R does not change significantly outside the relatively small region where $\sigma = O(1)$, this gives us

$$\frac{L_e}{R_e} + \frac{L_b}{R_b} = L_e + L_b,$$

where R_e and R_b are the respective radii of the axon far into the eye or far along the optic nerve. Letting $\gamma = \frac{L_e}{L_e + L_b}$, the proportion of the total length of the axon in the eye, this gives a boundary condition on R of

$$\gamma \lim_{\sigma \to -\infty} \frac{1}{R} + (1 - \gamma) \lim_{\sigma \to \infty} \frac{1}{R} = 1,$$

assuming $L_e/L \to -\infty$ and $L_b/L \to \infty$.

In the regions far from the lamina cribrosa there is an equilibrium between external and internal pressures and therefore no flow. Mathematically, this can be expressed as

$$\lim_{\sigma \to -\infty} \frac{dP}{d\sigma} = \lim_{\sigma \to \infty} \frac{dP}{d\sigma} = 0,$$

where again the limits on σ are understood as $L_e/L \to -\infty$ and $L_b/L \to \infty$.

2.4 Summary of model

If we assume the axon to be a cylinder of constant radius, the flow of water along the axon may be described by the nondimensional equation

$$\frac{d^2P}{d\sigma^2} - P = -P_{\text{ext}}(\sigma) - \tilde{\Pi}, \tag{10}$$

obtained by setting R and α to 1 in equation (6). In this equation, P represents the internal pressure along the axon, σ is a measure of distance along the length along the axon, $\tilde{\Pi}$ is the osmotic pressure difference across the axonal membrane and $P_{\text{ext}}(\sigma)$ represents the external hydrostatic pressure, defined by

$$P_{\text{ext}}(\sigma) = \begin{cases} 1, & \sigma < 0; \\ 0, & \sigma > 0. \end{cases}$$

We will solve equation (10) subject to the boundary conditions

$$\lim_{\sigma \to -\infty} \frac{dP}{d\sigma} = \lim_{\sigma \to \infty} \frac{dP}{d\sigma} = 0. \tag{11}$$

In this case, using equation (8) we find that the flux of fluid along the axon (in the direction of increasing σ) is given simply by

$$F = -\frac{dP}{d\sigma}. \tag{12}$$

If we allow the radius of the axon to vary, but make the simplifying assumptions described in Section 2.3, we find that the flow and radial changes are described by the nondimensional system of equations

$$\frac{d}{d\sigma}\left(R^5\frac{dP}{d\sigma}\right) + P_{\text{ext}}(\sigma) + \tilde{\Pi} - P = 0,$$

$$\frac{d}{d\sigma}(R(P - P_{\text{ext}}(\sigma))) - \frac{R}{2}\frac{dP}{d\sigma} = 0;$$

where P, σ, $P_{\text{ext}}(\sigma)$ and $\tilde{\Pi}$ are defined as above and R is the varying radius. To solve this, we use the same boundary conditions on P as given in equation (11) and the following boundary condition on R:

$$\gamma \lim_{\sigma\to-\infty}\frac{1}{R} + (1-\gamma)\lim_{\sigma\to\infty}\frac{1}{R} = 1.$$

As before, using equation (8) we find that the flux of fluid along the axon (in the direction of increasing σ) is given by

$$F = -R^5\frac{dP}{d\sigma}. \tag{13}$$

3 Analysis and interpretation of the model

3.1 Analysis of simplified model

As given in Section 2.4, the simplified model for constant R defined by (10,11) can be solved analytically. We consider two regions: Region I where $\sigma < 0$ and $P_{\text{ext}} = 1$ and Region II where $\sigma > 0$ and $P_{\text{ext}} = 0$. As (10) involves the second derivative of P, we require both P and $\frac{dP}{d\sigma}$ to be continuous throughout. By inspection, the solution in Region I will have the form

$$P^I = Ae^{\sigma} + Be^{-\sigma} + \tilde{\Pi} + 1, \qquad \sigma < 0;$$

while the solution in Region II will have the form

$$P^{II} = Ce^{\sigma} + De^{-\sigma} + \tilde{\Pi}, \qquad \sigma > 0;$$

where A, B, C and D are constants to be determined.

In order to satisfy the boundary conditions, we discard the exponentially growing terms ($Be^{-\sigma}$ for $\sigma < 0$ and Ce^{σ} for $\sigma > 0$) yielding

$$P^I = Ae^{\sigma} + \tilde{\Pi} + 1,$$

$$P^{II} = De^{-\sigma} + \tilde{\Pi};$$

and subsequently

$$\frac{dP^I}{d\sigma} = Ae^{\sigma},$$

$$\frac{dP^{II}}{d\sigma} = -De^{-\sigma}.$$

As P and $\frac{dP}{d\sigma}$ must be continuous at $\sigma = 0$, we can equate the limits of P^I and P^{II} as σ approaches 0, and similarly for the derivatives. This gives

$$A + \tilde{\Pi} + 1 = D + \tilde{\Pi}$$
$$A = -D,$$

and hence

$$A = -1/2 \qquad D = 1/2.$$

Substituting back into the equations for P^I and P^{II}, we find that our complete solution for P is

$$P = \begin{cases} \tilde{\Pi} + 1 - \frac{e^{\sigma}}{2} & \sigma < 0, \\ \tilde{\Pi} + \frac{e^{-\sigma}}{2} & \sigma > 0. \end{cases} \tag{14}$$

Substituting this into the definition of flow given in equation (12), we also find that

$$F = \begin{cases} \frac{e^{\sigma}}{2} & \sigma < 0, \\ \frac{e^{-\sigma}}{2} & \sigma > 0. \end{cases} \tag{15}$$

These are illustrated graphically in Figure 3 below.

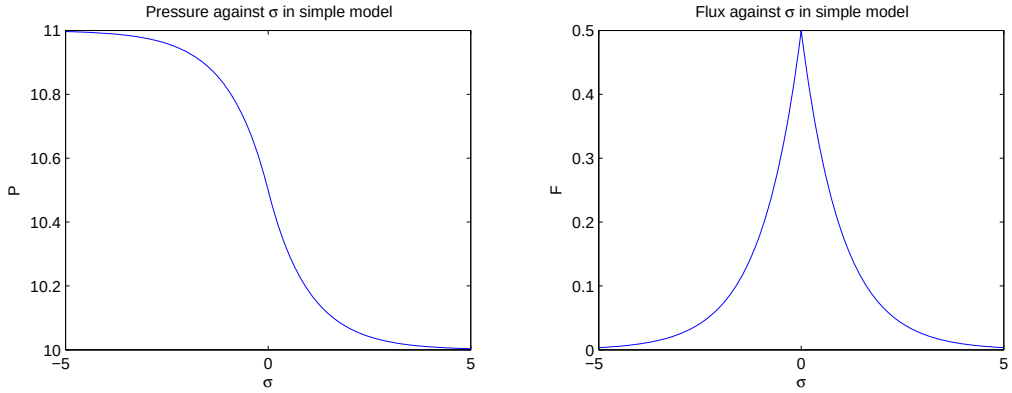

Figure 3: Solution to the model with R constant - P and F plotted against σ with the constant Π taken to be 10.

3.2 Interpreting the result for F

One important observation from our solution is that the flux of axoplasm, F, reaches its maximum value of $\frac{1}{2}$ when $\sigma = 0$. This indicates that the flow is fastest at the point where the axon passes through the lamina cribrosa. Furthermore, we can reverse the nondimensionalisation to find the maximum flux in SI units using equation (9). If $F_{\max}$ is the dimensional maximum flux, we find that

$$F_{\max} = \frac{\pi \bar{r}^4 (p_e - p_b)}{16 \mu L}.$$

Dividing by the cross-sectional area of the tube, we find that the average velocity of water along the axon at the point of maximum flux is given by

$$V_{\max} = \frac{\bar{r}^2 (p_e - p_b)}{16 \mu L} = \frac{L \kappa (p_e - p_b)}{\bar{r}},$$

as $\alpha = \frac{\bar{r}^3}{16 \mu \kappa L^2} = 1$.

As mentioned in Section 1, we hypothesise that the flow of water through the axon is fast enough that the lamina cribrosa effectively becomes a one-way valve for biologically active

molecules, cutting off communication between the two halves of the axon and ultimately depriving one end of the axon of substances necessary for cell survival. In order to evaluate this hypothesis, we must determine the Peclet number of the flow, which compares the rate of directed flow with the rate of random diffusion. The Peclet number Pe is defined by

$$Pe = \frac{V_{\max} L^*}{D},$$

where L^* is an appropriate characteristic length and D is the diffusivity of the material being considered. If the Peclet number is much larger than 1, it indicates that diffusion is not significant and practically all of the motion of particles is in the direction of flow.

In this case, it seems most sensible to take L^* to be the characteristic length L already used, although this may cause the Peclet number to be overestimated. It has been difficult to find an appropriate value for the diffusivity of proteins along the optic nerve, but we will use $D = 10^{-7}$ cm^2 sec^{-1}, which is characteristic of protein diffusivity in the lens of the eye [7] and also haemoglobin diffusivity in blood [8]. For the pressure difference between the eye and the CSF, we use a value of 20 mmHg as being typical of acute angle-closure glaucoma, [1].

In SI units, this gives us the following values for our relevant constants:

$$\bar{r} = 2.5 \times 10^{-7} \text{ m}, \qquad p_e - p_b = 2.7 \times 10^3 \text{ Pa}, \qquad \mu = 8.9 \times 10^{-4} \text{ Pa s},$$
$$L = 3 \times 10^{-4} \text{ m}, \qquad \kappa = 10^{-11} \text{ m s}^{-1} \text{ Pa}^{-1}, \qquad D = 10^{-11} \text{ m}^2 \text{ s}^{-1}.$$

Using these values, we get a maximum flux of

$$F_{\max} = 8 \times 10^{-18} \text{ m}^3 \text{ s}^{-1},$$

and a maximum velocity of

$$V_{\max} = 4 \times 10^{-5} \text{ m s}^{-1},$$

yielding a Peclet number of

$$Pe = 10^3.$$

Although this is a maximum value for Pe, we note that it is significantly larger than one, indicating that the flow along the axon should be sufficiently fast to prevent proteins and other large molecules from being able to move against the main flow. Interestingly, if the pressure difference is less than 1 mmHg it seems unlikely that the axoplasmic flow would be seriously disrupted. This is consistent with the observation that occasional small pressure imbalances do not lead to glaucoma - a large pressure difference needs to be held for a lengthy period of time in order to induce significant cell death.

The value for the Peclet constant given here is subject to accumulated errors from estimating parameters, and the actual value of Pe may differ from this by a couple of orders of

magnitude. Further experimentation is necessary in order to determine more realistic values for the collection of constants given above. Similarly, the axon may contain active transport mechanisms that could work to reduce the effect of the internal flow. Further investigation is necessary in order to determine conclusively whether our proposed mechanism of cell death (ie. the presence of a flow which prevents the proper distribution of biologically active molecules from being maintained) is valid.

3.3 Analysis of full model

As given in Section 2.4, we wish to solve the equations

$$\frac{d}{d\sigma}\left(R^5\frac{dP}{d\sigma}\right) + P_{\text{ext}}(\sigma) + \tilde{\Pi} - P = 0, \tag{16}$$

$$\frac{d}{d\sigma}(R(P - P_{\text{ext}}(\sigma))) - \frac{R}{2}\frac{dP}{d\sigma} = 0; \tag{17}$$

subject to the following boundary conditions:

$$\lim_{\sigma\to-\infty}\frac{dP}{d\sigma} = \lim_{\sigma\to\infty}\frac{dP}{d\sigma} = 0 \tag{18}$$

$$\gamma\lim_{\sigma\to-\infty}\frac{1}{R} + (1-\gamma)\lim_{\sigma\to\infty}\frac{1}{R} = 1. \tag{19}$$

The function $P_{\text{ext}}(\sigma)$ is defined by

$$P_{\text{ext}}(\sigma) = \begin{cases} 1 & \sigma < 0, \\ 0 & \sigma > 0. \end{cases} \tag{20}$$

Also, the flux of water along the axon is given by

$$F = -R^5\frac{dP}{d\sigma}, \tag{21}$$

and the tension along the body of the axon (as derived in Appendix C and given in equation (5)) is given by

$$T = R(P - P_{\text{ext}}(\sigma)). \tag{22}$$

We notice that equations (16) and (17) contain the σ derivatives of P, F and T but not the σ derivative of R. This means that although we require that P, F and T are continuous for all σ, it is not necessary that R is continuous, and it is possible that R will jump at $\sigma = 0$.

We cannot solve the system of equations above analytically, but it is possible to find an asymptotic solution for the case where $\tilde{\Pi}$ is large. Recalling that $\tilde{\Pi} = \frac{\Pi}{p_e - p_b}$, we notice

that $\tilde{\Pi}$ large corresponds to a case where the osmotic pressure difference across the axonal membrane is much larger than the pressure difference between the eye and the CSF in the optic nerve. This will be the case when $p_e - p_b$ is close to zero, indicating a situation where the glaucoma or papilloedema is not severe. Furthermore, although we do not have experimental values for Π, we expect that it is significantly larger than $p_e - p_b$, because it can be shown that if this is not the case the entire optic nerve is liable to being completely and catastrophically crushed by the changing pressure across the lamina cribrosa. This is inconsistent with the observation that glaucoma and papilloedema proceed gradually over a period of many years.

Let $\tilde{\Pi} = \frac{1}{\eta}$ where $0 < \eta \ll 1$, and let P and R be expanded as

$$P = \frac{P_{-1}}{\eta} + P_0(\sigma) + \eta P_1(\sigma) + \dots$$
$$R = R_0 + \eta R_1(\sigma) + \dots,$$

where P_i and R_i are all $O(1)$.

We notice that the leading-order terms are taken to be constant while the other terms are functions of σ. This is because if we take $p_e - p_b$ all the way to zero (corresponding to $\eta = 0$), we expect a solution where the radius and pressure profiles are uniform across the length of the axon. Further checking will show that the solutions obtained on the assumption of spatially-uniform P_{-1} and R_0 are consistent with all of the relevant equations. Hence, by the uniqueness properties of well-posed differential equations, we can be confident that these solutions are correct.

Substituting our expressions for P and R above into equations (16) and (17) and only considering terms of order $\frac{1}{\eta}$, we obtain the following system:

$$\frac{d}{d\sigma}\left(R_0^5 \frac{dP_{-1}}{d\sigma}\right) + 1 - P_{-1} = 0, \tag{23}$$

$$\frac{d}{d\sigma}(R_0 P_{-1}) - \frac{R_0}{2}\frac{dP_{-1}}{d\sigma} = 0. \tag{24}$$

Similarly, subsituting in P and R to equations (18) and (19) and considering only terms of order $\frac{1}{\eta}$ in (18) and only those of order 1 in equation (19) we obtain the following boundary conditions:

$$\lim_{\sigma\to-\infty} \frac{dP_{-1}}{d\sigma} = \lim_{\sigma\to\infty} \frac{dP_{-1}}{d\sigma} = 0 \tag{25}$$

$$\gamma \lim_{\sigma\to-\infty} \frac{1}{R_0} + (1-\gamma) \lim_{\sigma\to\infty} \frac{1}{R_0} = 1. \tag{26}$$

With the assumpton that P_{-1} and R_0 are constant functions of σ, we find that equations (24) and (25) are identically true for all possible values of P_{-1} and R_0. Furthermore, using this assumption we find from equation (23) that

$$P_{-1} = 1$$

and from equation (26) that

$$R_0 = 1.$$

Thus $P_{-1} = 1$ and $R_0 = 1$ satisfy equations (23) to (26) and give us our leading-order solution for P and R.

Now, we consider the $O(1)$ terms of equations (16) to (18) and the $O(\eta)$ terms of (19) to find the first corrections to our leading-order solutions. This gives us the following system:

$$\frac{d^2 P_0}{d\sigma^2} + P_{\text{ext}}(\sigma) - P_0 = 0 \tag{27}$$

$$\frac{d}{d\sigma}\left(R_1 + P_0 - P_{\text{ext}}(\sigma)\right) - \frac{1}{2}\,\frac{dP_0}{d\sigma} = 0, \tag{28}$$

subject to boundary conditions

$$\lim_{\sigma\to-\infty} \frac{dP_0}{d\sigma} = \lim_{\sigma\to\infty} \frac{dP_0}{d\sigma} = 0 \tag{29}$$

$$\gamma \lim_{\sigma\to-\infty} R_1 + (1-\gamma) \lim_{\sigma\to\infty} R_1 = 0. \tag{30}$$

We notice that P_0 completely decouples from R_1, and furthermore we find that solving equations (27) and (29) is completely analogous to solving the simplified model described in Section 3.1. Hence, we find that

$$P_0 = \begin{cases} 1 - \frac{e^{\sigma}}{2} & \sigma < 0, \\ \frac{e^{-\sigma}}{2} & \sigma > 0. \end{cases}$$

Substituting this into equation (28), we find that in Region I where $\sigma < 0$ the solution for R_1 must satisfy

$$\frac{dR_1^I}{d\sigma} - \frac{e^{\sigma}}{4} = 0,$$

while in Region II where $\sigma > 0$ it must satisfy

$$\frac{dR_1^{II}}{d\sigma} - \frac{e^{-\sigma}}{4} = 0.$$

Hence,

$$R_1 = \begin{cases} A + \frac{e^{\sigma}}{4} & \sigma < 0, \\ B - \frac{e^{-\sigma}}{4} & \sigma > 0. \end{cases} \tag{31}$$

In order to find the values of A and B, we apply an appropriate matching condition at $\sigma = 0$ in addition to the boundary condition on R_1 given in (30). For the matching condition at $\sigma = 0$, we note that R is not necessarily continuous at $\sigma = 0$. Instead, since $P_{\text{ext}}(\sigma)$ is discontinuous at $\sigma = 0$, R_1 must also be discontinuous at $\sigma = 0$ in order to ensure that the expression $R_1 + P_0 - P_{\text{ext}}(\sigma)$ in equation (28) is differentiable. Since P_{ext} decreases by 1 at $\sigma = 0$ and P_0 is continuous everywhere, it follows that R_1 must decrease by 1 to make $R_1 + P_0 - P_{\text{ext}}(\sigma)$ continuous. Hence,

$$\lim_{\sigma \to 0^-} R_1 - 1 = \lim_{\sigma \to 0^+} R_1$$

$$A + \frac{1}{4} - 1 = B - \frac{1}{4},$$

yielding the result that

$$A = B + \frac{1}{2}.$$

Substituting equation (31) into the boundary condition in (30), we find that

$$\gamma A + (1 - \gamma)B = 0$$

$$\gamma \left(B + \frac{1}{2} \right) + (1 - \gamma)B = 0$$

$$\frac{\gamma}{2} + B = 0,$$

giving us the result that

$$A = \frac{1 - \gamma}{2}, \qquad B = \frac{-\gamma}{2}.$$

Substituting these back into equation (31) gives

$$R_1 = \begin{cases} \frac{1-\gamma}{2} + \frac{e^{\sigma}}{4} & \sigma < 0, \\ \frac{-\gamma}{2} - \frac{e^{-\sigma}}{4} & \sigma > 0. \end{cases}$$

Combining all of the results and rewriting η in terms of $\tilde{\Pi}$, we find that our asymptotic solutions for P and R are given by

$$P = \begin{cases} \tilde{\Pi} + 1 - \frac{e^{\sigma}}{2} + O\left(\tilde{\Pi}^{-1}\right) & \sigma < 0, \\ \tilde{\Pi} + \frac{e^{-\sigma}}{2} + O\left(\tilde{\Pi}^{-1}\right) & \sigma > 0; \end{cases} \tag{32}$$

and

$$R = \begin{cases} 1 + \tilde{\Pi}^{-1}\left(\frac{1-\gamma}{2} + \frac{e^{\sigma}}{4}\right) + O\left(\tilde{\Pi}^{-2}\right) & \sigma < 0, \\ 1 + \tilde{\Pi}^{-1}\left(\frac{-\gamma}{2} - \frac{e^{-\sigma}}{4}\right) + O\left(\tilde{\Pi}^{-2}\right) & \sigma > 0. \end{cases} \tag{33}$$

Furthermore, we can use equation (21) to find that

$$\begin{aligned} F &= R^5 \frac{dP}{d\sigma} \\ &= \tilde{\Pi}\, R_0^5\, \frac{dP_{-1}}{d\sigma} + 5R_0^4\, R_1\, \frac{dP_{-1}}{d\sigma} + R_0^5\, \frac{dP_0}{d\sigma} + O\left(\tilde{\Pi}^{-1}\right), \end{aligned}$$

and hence (with the appropriate substitutions)

$$F = \begin{cases} \frac{e^{\sigma}}{2} + O\left(\tilde{\Pi}^{-1}\right) & \sigma < 0, \\ \frac{e^{-\sigma}}{2} + O\left(\tilde{\Pi}^{-1}\right) & \sigma > 0. \end{cases} \tag{34}$$

Interestingly, this means that to $O(1)$ the solutions for P and F in the full model are the same as for the constant radius model. This justifies the constant radius simplification for finding the rate of flow in the case where the osmotic pressure difference is significantly larger than $p_e - p_b$. To leading order, the full model leads to the same analysis of flow relative to diffusion as given in Section 3.2 for the simplified model.

We developed MATLAB code to run simulations of the full model and compared the results obtained from this code with the asymptotic solutions given above. The MATLAB code was written to drive the package bvp4c, which solves boundary value problems using a relaxation method. Results of the numerics are shown (with a comparison to the asymptotic solution) in Figure 4.

3.4 Interpreting the result for R

One of the more peculiar features of this result is that the radius of the axon is larger on the left-hand side of the lamina cribrosa where the external pressure is greater and smaller on the right-hand side of the lamina cribrosa where the external pressure is smaller. Furthermore, this behaviour is exacerbated near the lamina cribrosa: the axon widens on the high-pressure side and narrows on the low-pressure side.

We can find the reasons for this strange behaviour by considering what the terms in equation (17) mean. Firstly we note that tension is defined by

$$T = R(P - P_{\text{ext}}(\sigma)).$$

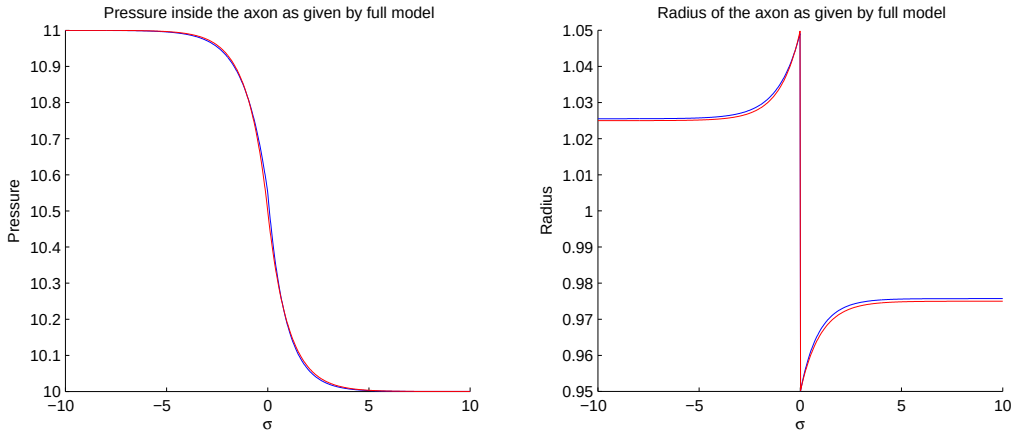

Figure 4: Solution to the full model - P and R plotted against σ with the $\tilde{\Pi} = 10$ and $\gamma = \frac{1}{2}$. The red line shows the asymptotic solutions (as given in equations (32) and (33)) and the blue line shows the numeric solution of the full model.

This can be physically interpreted by considering tension and pressure around a membranous hoop. If we have a hoop being held open by a constant pressure difference and we increase the tension of the membrane, the radius must increase because the pressure needs to be applied over a larger area to get the larger tension.

Substituting in our definition of tension, equation (17) can be rewritten as follows:

$$\frac{dT}{d\sigma} - \frac{R}{2}\frac{dP}{d\sigma} = 0. \tag{35}$$

As $\sigma < 0$ corresponds to the high pressure region (the eye) and $\sigma > 0$ corresponds to the low pressure region (the optic nerve and brain), we expect $\frac{dP}{d\sigma}$ to be consistently negative and this is indeed what we see in Figure 4. Since R must always be positive for realistic results, this means that

$$\frac{dT}{d\sigma} < 0$$

for all σ.

That is, tension is greater on the high pressure side than on the low pressure side. One way to think of this is that the shear forces in the high pressure region are stretching the membrane, pulling it towards the lamina cribrosa, while the shear forces in the low pressure side are compressing the membrane, pushing it away from the lamina cribrosa. The net result is that higher external pressure corresponds to higher tension.

Far from the lamina cribrosa, the hydrostatic and osmotic pressures will be in equilibrium.

That is, as $\sigma \to \pm\infty$ we find that $P - P_{\text{ext}} \to \tilde{\Pi}$. However, as defined before,

$$T = R(P - P_{\text{ext}}),$$

meaning that as $\sigma \to \pm\infty$ the radius will be given by

$$R = \frac{T}{\tilde{\Pi}}.$$

Thus, since higher external pressure corresponds to higher tension (as described before), we find that the radius is greater on the side where the external pressure is greater.

The 'kink' in the radius graph around the lamina cribrosa is due to a similar effect. We note from the asymptotic solution that $R \approx 1$ throughout. Hence, equation (35) can be rewritten as

$$\frac{dT}{d\sigma} \approx \frac{1}{2}\frac{dP}{d\sigma}.$$

This means that as we go towards the lamina cribrosa from the high pressure side ($\sigma \to 0^-$), the tension only decreases half as fast as pressure does. Since

$$R = \frac{T}{P - P_{\text{ext}}},$$

this means that there is a net increase in R as σ increases towards 0. A similar argument can be used to explain the behaviour of R as $\sigma \to 0^+$.

Essentially, the unusual behaviour of R stems directly from our leading order expression for tension obtained in Appendix C. It would be interesting to determine whether this behaviour is consistent with the six-equation model given at the end of Section 2.2 or whether the simplification to the two-equation model involved the loss of terms which are actually significant.

Lastly, we note that it is possible to draw a parallel between the strange behaviour observed in these results and the inflation of a balloon. As a balloon is inflated, the tension in the rubber membrane remains fairly constant. Since a spherical membrane is governed by similar equations to the ones derived here, this means that as the radius of the balloon increases, the pressure inside *decreases*. This leads to an interesting experiment in which two balloons of different sizes are connected by a tube: the high pressure in the smaller balloon means that it deflates into the larger balloon.

Hence, if two balloons of exactly same size are connected by a tube, the pressures will be in an unstable equilibrium. Any perturbation in the pressures will cause one balloon to deflate completely into the other one. This raises the worrying possibility that the deformation result that we have obtained is also an example of an unstable solution to the membrane equations. It may be necessary to construct a model which includes time dependence in order to investigate the stability (and hence reliabiity) of the results obtained.

4 Conclusions

4.1 Summary of work done

We have constructed a model of how the axons of retinal ganglial cells respond to the difference between the intraocular pressure and the CSF pressure that is characteristic of glaucoma and papilloedema. As described in Section 2.1, our model uses Poiseuille's law to describe flow along the axon, taking into account water driven through the membrane surrounding the axon by a difference in hydrostatic and osmotic pressures across the membrane. In addition to our model of fluid flow in the axon, we developed a model of the mechanical deformation of the axon in response to hydrostatic pressure differences, and shear forces induced by flow, as described in Section 2.2.

We were able to simplify the full model obtained at the end of Section 2.2 by nondimensionalising the model and discarding terms that did not make a significant contribution to the model, given the geometry of the axon as a long, thin tube. This greatly simplified the model down to a system of two equations, (6) and (7), described in Section 2.3. A further simplification of the model was to remove the membrane mechanics by taking the radius of the axon to be constant along its length. This model can be solved analytically, but may not capture some of the important details of the axon's response to the pressure difference between the eye and the CSF.

After solving the simplified constant radius model (Section 3.1), we considered how to interpret the result obtained for the flux of fluid along the axon. This work, detailed in Section 3.2, is the most important accomplishment of the study group. We were able to demonstrate that the flux of water along the axon is greatest at the point where the axon passes through the lamina cribrosa, and that the flow at that point is sufficiently fast to make it impossible for large proteins to diffuse in the opposite direction to the prevailing flow. This gives us a novel mechanism for the death of axons in glaucoma and papilloedema - they die because the cell is unable to maintain the distribution of essential proteins throughout the cell that is necessary for survival. Further experimental work is necessary to determine whether this is indeed the case.

We also analysed the full model obtained in Section 2.3. Here, asymptotic methods proved particularly fruitful with the expansion in large $\tilde{\Pi}$ yielding the results given in Section 3.3 and comparing very well with numeric solutions using MATLAB. Interestingly, to leading order the results for flux obtained from the full model were the same as for the simplified model. Hence, there was no need for further interpretation of the fluxes; Section 3.2 applies for the full model as well as the simplified model.

However, the solutions obtained for the changing radius of the axon seem unrealistic. The

axon appears to be wider in the region where it is under a higher external pressure and is narrower where it is under a lower external pressure. Section 3.4 describes how this arises from the equations used. It is not yet clear whether the strange solution for the changing radius is physically realistic or a property of how the model was constructed.

4.2 Possible extensions to the model

The models as described in this report have the advantage of not containing many parameters that cannot be reliably estimated from the results in the published literature. However, there are some advantages to considering more complicated models where not all of the data is readily available. Here are some examples of possible extensions to the model developed during the study group:

Full mechanical model
It may be interesting to find numerical solutions to the full mechanical model derived in Section 2.2. The difficulty with this model would be finding realistic values for $\tilde{B}$ and boundary conditions on the variables. On the other hand, this might be necessary in order to determine whether the result for R described in Section 3.4 is realistic or whether some important features have been lost in the simplification. For one thing, R would now be contnuous, because the derivative of R appears in the full system of equations. Furthermore, although our work is based on the assumption that $\tilde{B}$ is not large, it is possible that this assumption is flawed and $\tilde{B}$ is large enough for the full system to be unavoidable.

Time dependency
Developing a time-dependent model of membrane mechanics would potentially be extremely complicated. However, this step may be necessary in order to determine whether the equilibrium solutions that we have obtained are stable and physically realistic, or unstable and unrealistic. A time dependent model should only be constructed if the full mechanical model is unable to clarify the unusual solution for R obtained.

Including the lamina cribrosa
The present model treats the lamina cribrosa as being an infinitesimally thin layer in which the external pressure jumps suddenly. However, this is not actually the case, since the length of the axon in the lamina cribrosa is quite substantial compared to the length of the axon over which flow takes place. Hence, it would be interesting to see what impact including the lamina cribrosa would have on the behaviour of the model. The main difficulty with this is that it is not clear what form a model including the lamina cribrosa should take. One option would be to make the transition between the two external pressures more gradual. On the other hand, the lamina cribrosa is basically solid, so the way it exerts pressure on the axon will be different to the hydrostatic pressures experienced in the eye and along the optic nerve. This problem deserves further consideration.

A bundle of axons
In glaucoma and papilloedema, peripheral vision is affected before central vision, meaning that axons near the edge of the optic nerve are affected before those in the middle of the nerve. One possible reason for this based on our model is that the axons in the middle of the nerve are shielded from the sudden pressure gradient by those around them. It would be interesting to construct a model of a bundle of axons to investigate whether this effect is significant enough to explain the observed behaviour.

Advection of proteins
The main extension that we considered during the study group was the advection of proteins along the axon. As discussed in Section 1.2, an osmotic pressure difference between the axon and the surrounding space exists because of dissolved proteins that are present in the axon but not outside it. This means that if there is a mechanism sweeping proteins along the axon, it is likely to affect the osmotic force balance; in terms of our model, Π is no longer a constant but is dependent on the concentration of protein. This extended model would need to include terms to account for the creation of proteins by the cell, loss of proteins as they are used by the cell and internal active transport of proteins. Despite the complexity that this introduces, it would be interesting to see the effects of the flow we identified on the osmotic forces, which could potentially have ramifications for the changing radius of the axon. Interestingly, we note that allowing the osmotic pressure to change would serve to increase the pressure differences experienced across the axonal membrane and speed up flow.

Bending of the axon
The dominant theories that currently exist as to how axon death occurs involve the mechanical squeezing, pinching and bending of the axons. We have developed a novel theory for axon death involving internal flow, but we have not been able to investigate the original mechanical theories of axon death. It would be useful to be able to develop models of these theories in order to compare and contrast them with the models obtained in this study.

4.3 Future work

We have developed an interesting and novel model of glaucoma and papilloedema that points to a mechanism of axon death that is different to what appears in the biological literature. Apart from the possible extensions to the model described above, the most constructive step forward is to work with biologists and clinicians to obtain experimental evidence that will support or refute our model. In aid of this, the next step should be to publish a peer-reviewed paper on our model and to actively approach people with experimental expertise who could collaborate on testing the model. This Study Group project was a fine example of how mathematics and medicine can inform and enrich each other and will hopefully lead to further productive collaborations and practical results.

References

[1] J. B. Jonas, E. Berenshtein, and L. Holbach. Anatomic relationship between lamina cribrosa, intraocular space, and cerebrospinal fluid space. *Investigative Ophthalmology and Visual Science*, 44:5189–5195, 2003.

[2] F. F. Vargas. Filtration coefficient of the axon membrane as measured with hydrostatic and osmotic methods. *The Journal of General Physiology*, 51:13–27, 1968.

[3] C. S. Spyropoulos. Osmotic relations of nerve fiber. *Journal of Membrane Biology*, 32:19–32, 1977.

[4] S.P. Timoshenko and S. Woinowsky-Krieger. Theory of plates and shells. *Engineering Societies Monographs, New York: McGraw-Hill, 1959, 2nd ed.*, 1959.

[5] D. C. Pamplona and C. R. Calladine. The mechanics of axially symmetric liposomes. *J. Biomech. Eng.*, 115:149–159, 1993.

[6] Preston S.P. *Mathematical models of cell motility, proliferation, and mechanics.* PhD thesis, University of Nottingham, 2006.

[7] T. Tanaka and C. Ishimoto. In vivo observation of protein diffusivity in rabbit lenses. *Investigative Ophthalmology and Visual Science*, 16:135–140, 1977.

[8] J. D. Murray. *Mathematical Biology*, volume 1. Springer-Verlag, Berlin, 3rd edition, 2002.

[9] E. A. Evans and R. Skalak. *Mechanics and Thermodynamics of Biomembranes.* CRC Press, Boca Raton, FL, 1980.

[10] C. Pozrikidis. Deformed shapes of axisymmetric capsules enclosed by elastic membranes. *J. Eng. Math.*, 45:169–182, 2003.

[11] K. H. Parker and C. P. Winlove. The deformation of spherical vesicles with permeable, constant-area membranes: application to the red blood cell. *Biophys. J.*, 77:3096–3107, 1999.

Appendix A

Mathematical detail for flow equations

The Navier-Stokes equations are given as follows:

$$\frac{\partial u}{\partial z} + \frac{1}{r}\,\frac{\partial}{\partial r}(rv) = 0, \tag{36}$$

$$\frac{\partial P}{\partial r} = 0, \tag{37}$$

$$-\frac{\partial P}{\partial z} + \frac{\mu}{r}\,\frac{\partial}{\partial r}\left(r\frac{\partial u}{\partial r}\right) = 0. \tag{38}$$

¿From equation (37), we find that P depends only on z. This makes it easy for us to integrate equation (38) with respect to r. Let $R(z)$ be the radius of the tube (that is, the radial coordinate of the boundary). Then, at a general point $z = z^*$ we have

$$\mu\frac{d}{dr}\left(r\frac{du(z^*,r)}{dr}\right) = r\left.\frac{dP}{dz}\right|_{z^*}$$

$$\mu\frac{du(z^*,r)}{dr} = \frac{r}{2}\left.\frac{dP}{dz}\right|_{z^*} + \frac{A}{r}$$

$$u(z^*,r) = \frac{r^2}{4\mu}\left.\frac{dP}{dz}\right|_{z^*} + A\ln r + B.$$

We can find the constants of integration A and B by noting that we want finite velocities when $r = 0$ (meaning that $A = 0$) and that there is zero velocity on the wall of the pipe so that

$$B = -\frac{R^2}{4\mu}\left.\frac{dP}{dz}\right|_{z^*}.$$

Generalising to all z, this gives the following expression for velocity down the pipe:

$$u(z,r) = \frac{r^2 - R^2}{4\mu}\,\frac{dP}{dz}. \tag{39}$$

In order to now find the total flux of fluid, F, at any point along the pipe, we must integrate

equation (39) across a cross-section. That is,

$$\begin{aligned} F &= \int_0^R 2\pi r u(r,z)\, dr \\ &= \int_0^R \frac{\pi(r^3 - rR^2)}{2\mu} \frac{dP}{dz}\, dr \\ &= \left(\frac{\pi R^4}{8\mu} - \frac{\pi R^4}{4\mu}\right)\frac{dP}{dz} \\ &= -\frac{\pi R^4}{8\mu}\frac{dP}{dz}. \end{aligned} \tag{40}$$

This equation is known as Poiseuille's law, and relates the average rate of flow through a pipe to the pressure gradient and the radius of the pipe.

We can also integrate equation (36) across the radius of the tube to effectively get a mass conservation equation for our system. Recalling that R is a function of z, we firstly use equation (39) to find that

$$\begin{aligned} \frac{\partial u}{\partial z} &= \frac{r^2 - R^2}{4\mu}\frac{d^2P}{dz^2} + \frac{\partial}{\partial z}\left(\frac{r^2 - R^2}{4\mu}\right)\frac{dP}{dz} \\ &= \frac{r^2 - R^2}{4\mu}\frac{d^2P}{dz^2} - \frac{R}{2\mu}\frac{dP}{dz}\frac{dR}{dz} \end{aligned}$$

Hence, from (36) we find that

$$\begin{aligned} -\frac{\partial}{\partial r}(rv) &= \frac{r(r^2 - R^2)}{4\mu}\frac{d^2P}{dz^2} - \frac{Rr}{2\mu}\frac{dP}{dz}\frac{dR}{dz} \\ v &= -\frac{r^3 - 2R^2r}{16\mu}\frac{d^2P}{dz^2} + \frac{Rr}{4\mu}\frac{dP}{dz}\frac{dR}{dz} + \frac{C}{r}. \end{aligned}$$

In order to find the constant C, we note that we do not expect any flow perpendicular to the pipe along its central line, as this would violate the conservation of mass. This means that v must be 0 when r is 0, implying in turn that $C = 0$. Hence,

$$v(z,r) = -\frac{r^3 - 2R^2r}{16\mu}\frac{d^2P}{dz^2} + \frac{Rr}{4\mu}\frac{dP}{dz}\frac{dR}{dz}. \tag{41}$$

On the boundary of the tube, we expect the perpendicular velocity to be determined by the flow across the permeable membrane that surrounds the axon. If κ is the permeability of the axon expressed as a flux per unit of pressure difference and Δp is the difference in pressure across the boundary (including osmotic and hydrostatic pressures), we expect that

$$\kappa \Delta p = -v(z,R).$$

Substituting into equation (41), this gives

$$\kappa \Delta p = -\frac{R^3}{16\mu} \frac{d^2 P}{dz^2} - \frac{R^2}{4\mu} \frac{dP}{dz} \frac{dR}{dz}$$

$$\kappa \Delta p = -\frac{1}{R} \frac{d}{dz} \left(\frac{R^4}{16\mu} \frac{dP}{dz} \right).$$

Appendix B

Mathematical detail for membrane mechanics

We wish to construct an appropriate mechanical model to determine the equilibrium deformation of the axon membrane subjected to forces arising from a nonuniform external pressure applied to the axonal membrane. This membrane is taken to be axisymmetric around the z-axis, but with a varying radius along its length. Figure 5 shows some of the important features of our idealised axon. One significant parameter in our model is the angle ϕ between the tangent along the axonal membrane and the radius (as shown), which can be used to describe the rate at which the radius varies along the length of the axon. Significantly, we expect the change in the axon radius to be gradual over the length scale of the axon. This means that ultimately we can use the long wavelength approximation and take ϕ to be always close to $\frac{\pi}{2}$.

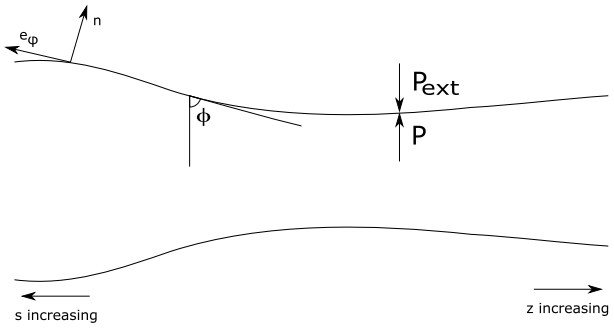

Figure 5: The angle ϕ shown on the axisymmetric axon with the hydrostatic pressures and the vectors $\mathbf{n}$ and $\mathbf{e}_\phi$. The vector $\mathbf{e}_\theta$ goes around the axon. Note that with the formulation used, the direction of z increasing is opposite to the direction of s increasing, [5].

In addition to ϕ, we need vectors $\mathbf{n}$, $\mathbf{e}_\theta$ and $\mathbf{e}_\phi$ to form a basis for our three dimensional space. The vector $\mathbf{n}$ is a taken to be the unit vector normal to the surface of the axon while $\mathbf{e}_\theta$ and $\mathbf{e}_\phi$ are both tangential to the surface of the membrane and are defined so that $\mathbf{e}_\theta$ is perpendicular to the z axis (going around the axon) while $\mathbf{e}_\phi$ is perpendicular to $\mathbf{e}_\theta$ and will be parallel with the z axis when the radius is constant. The vectors $\mathbf{n}$ and $\mathbf{e}_\phi$ are illustrated on Figure 5.

In order to find the equilibrium configuration of the axon, we must first consider the forces acting upon it. A difference in pressures between the fluid on the inside of the axon (at a pressure of P) and that on the outside (at a pressure of P_{ext}) gives rise to a normal force of $(P - P_{\text{ext}})\mathbf{n}$ per unit area. Flow down the axon also gives rise to a tangential stress $G\mathbf{e}_\phi$, where G is the shear rate on the membrane of the axon, defined by $G = -\frac{dP}{dz}$. In addition to these applied forces, we must consider the axon's resistance to deformation and the build-up

of internal stresses.

The theory used to deal with thin structures such as the axonal membrane is called shell theory (see, for example, [4]). In this theory, the stresses within the membrane are represented by *so-called* stress resultants; effectively the averaged stresses across the thickness of the structure. Along any particular elemental line length dl inscribed on the surface of the membrane we find that a tension (Tdl), a normal shear resultant (Q) and a moment ($\mathbf{M}dl$) will act.

In general, T, Q and $\mathbf{M}$ are functions of the orientation of the line element and can each be written in tensorial form. For the axisymmetric case, we need only consider the components of T and $\mathbf{M}$ in the $\mathbf{e}_\theta$ and $\mathbf{e}_\phi$ directions and need only consider the components of Q in the $\mathbf{e}_\phi$ direction. Following Pamplona and Calledine [5] (see [6] for a clear exposition), we use force and moment balances on an area element to derive three equations relating the five unknown stress resultants (T_θ, T_ϕ, Q_ϕ, M_θ and M_ϕ) as follows:

Axial force balance:

$$\frac{d}{ds}(RT_\phi) - T_\theta \cos\phi - \frac{d\phi}{ds} RQ_\phi = \frac{GR^2}{2},$$

Normal force balance:

$$\frac{d}{ds}(RQ_\phi) + \sin\phi T_\theta + RT_\phi \frac{d\phi}{ds} = (P - P_{\text{ext}})R,$$

Moment balance:

$$\frac{d}{ds}(M_\phi R) - M_\theta \cos\phi + RQ_\phi = 0.$$

It is important to note that all of these equations are written in terms of the arclength parameter s rather than the perpendicular distance along the axon, z. Following the work of Pamplona and Calledine [5], we note also that the system is constructed so that the direction of s increasing is the opposite to the direction of z increasing. Generally, s and z may be related by the equation

$$dz = -\sin\phi \, ds, \tag{42}$$

which simplifies to $z = -s$ in the case where $\phi \to \frac{\pi}{2}$ and hence $\sin\phi \to 1$.

The three equations above must be coupled with constitutive equations for the tension and bending moment. Researchers have used a variety of choices for these relations (see, for example, Evans and Skalak [9] and Pozrikidis [10]), but here we adopt those used by Pamplona and Calledine [5] and Parker and Winlove [11]; namely

$$T_\phi - T_\theta = H\left(\lambda_\theta - \lambda_\phi\right), \qquad M_\phi = M_\theta = B\left(\frac{d\phi}{ds} + \frac{\sin\phi}{R}\right),$$

where H is the the shear modulus, B is the bending modulus, λ_θ is the principle stretch in the θ direction and λ_ϕ that in the ϕ direction. The expression for M_ϕ and M_θ is derived from the assumption that the moment is isotropic and proportional to the total curvature of the membrane. Geometrically, it can be shown that $\frac{d\phi}{ds}$ and $\frac{\sin\phi}{R}$ respectively represent the principal curvatures in the ϕ and θ directions.

In the case where the membrane is inextensible (a good approximation for lipid bilayers), the principle stretches are related by $\lambda_\phi = 1/\lambda_\theta$. Moreover, if the membrane has an essentially fluid structure we expect the resistance to shear to be small so that the tensions may be considered to be isotropic, meaning that $T_\phi = T_\theta$.

Noting these constitutive assumptions, we can define $T = T_\phi = T_\theta$ and $M = M_\phi = M_\theta$ and visualise the various forces and moments acting on a small segment of the axon using Figure 6 (also shown as Figure 2 in the main document).

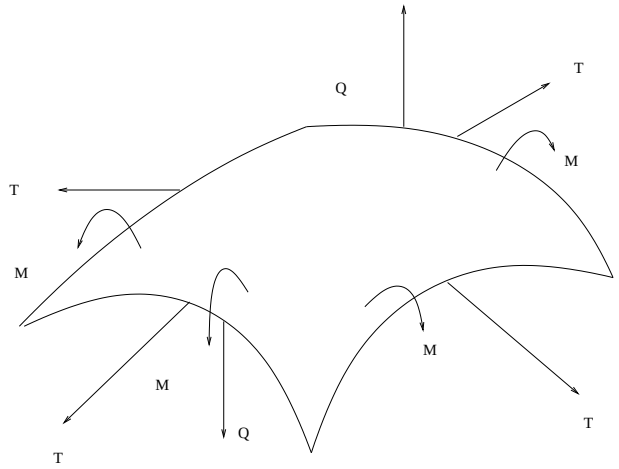

Figure 6: The tension T, bending moment M and normal shear resultant Q acting on a small element of the axon membrane. Together with the influence of the hydrostatic pressure difference across the membrane and the shear forces due to fluid flow along the axon, these forces define the shape that the membrane takes.

Thus, we obtain the following system of dimensional equations:

$$\begin{aligned}
\frac{d}{ds}(RT) - T\cos\phi - \frac{d\phi}{ds}RQ &= \frac{GR^2}{2}, \\
\frac{d}{ds}(RQ) + \sin\phi T + RT\frac{d\phi}{ds} &= (P - P_{\text{ext}})R, \\
\frac{d}{ds}(MR) - M\cos\phi + RQ &= 0, \\
M &= B\left(\frac{d\phi}{ds} + \frac{\sin\phi}{R}\right);
\end{aligned}$$

giving us four equations in six unknowns (R, ϕ, T, Q, M and P). In order to make the system well defined, we need two further equations. Firstly, we note that ϕ may be defined geometrically in terms of R by the equation

$$\frac{dR}{ds} = \cos\phi,$$

and secondly we recall that we need to couple flow equation (3) from Section 2.1 to the system. Noting the result given in (42), the flow equation can be rewritten in terms of s as

$$\kappa(P_{\text{ext}} + \Pi - P) = -\frac{1}{16\mu R\sin\phi}\,\frac{d}{ds}\left(\frac{R^4}{\sin\phi}\,\frac{dP}{ds}\right).$$

The next step is to rewrite the problem in terms of $\bar{s}$, the arclength parameterisation that would be obtained if the axon were deformed from its current state without stretching so that it had a constant radius of $\bar{r}$. This is explained and detailed back in Section 2.2.

Appendix C

Mathematical detail for nondimensionalisation

A summary of the nondimensionalisations is given as follows:

$$R = \bar{r}R^*, \qquad P = p_b + (p_e - p_b)P^*, \qquad T = \bar{r}(p_e - p_b)T^*,$$
$$Q = \bar{r}(p_e - p_b)Q^*, \qquad M = \bar{r}^2(p_e - p_b)M^*, \qquad \bar{s} = L\sigma.$$

This nondimensionalisation is explained in Section 2.3. We also define a dimensionless small parameter ϵ based on the scalings of R and $\bar{s}$. This ϵ is defined by

$$\epsilon = \frac{\bar{r}}{L}.$$

It is worth making an additional comment on the nondimensionalisation for pressure. Although our pressure scaling gives us a very simple expression for $P^*_{\text{ext}}(\bar{s})$, our use of $p_e - p_b$ in the pressure scale has the potential to cause problems when $p_e = p_b$. However, it may be shown that if P_{ext} is constant and equal to some $\hat{p}$, our complete dimensioned system of equations can be solved by $P = \Pi + \hat{p}$, $R = \hat{r}$ (where $\hat{r}$ can be determined from the boundary conditions), $T = \Pi\hat{r}$, $Q = 0$ and $M = \frac{B}{\hat{r}}$. Unfortunately, in our nondimensionalised system this corresponds to P^* going to infinity even though P is finite and well-behaved. While aware of this possibility and noting that it may be better to scale P to Π, we proceed with this nondimensionalisation, following the work done during the Study Group.

Together with our nondimensionalisation, we can incorporate the long-wave approximation mentioned earlier. That is, we are considering a situation where R only changes slowly across the axon and so $\phi \approx \frac{\pi}{2}$. This motivates us to define a new variable $\hat{\phi}$ so that $\phi = \frac{\pi}{2} - \frac{\bar{r}}{L}\hat{\phi} = \frac{\pi}{2} - \epsilon\hat{\phi}$ (using the same definition of ϵ as before). Hence, $\sin\phi \approx 1$ and $\cos\phi \approx \epsilon\hat{\phi}$.

Applying all of these changes (and omitting the higher order terms from the simplification

of $\cos\phi$ and $\sin\phi$), we can rewrite our governing equations as follows:

$$\epsilon R^* \frac{d}{d\sigma}(R^* T^*) - \epsilon \hat{\phi} T^* + \epsilon^2 R^{*2} Q^* \frac{d\hat{\phi}}{d\sigma} = \epsilon \frac{R^{*3}}{2} \frac{dP^*}{d\sigma}, \tag{43}$$

$$\epsilon R^* \frac{d}{d\sigma}(R^* Q^*) + T^* + \epsilon^2 R^{*2} T^* \frac{d\hat{\phi}}{d\sigma} = (P^* - P^*_{\text{ext}}) R^*, \tag{44}$$

$$\epsilon R^* \frac{d}{d\sigma}(R^* M^*) - \epsilon \hat{\phi} M^* + R^* Q^* = 0, \tag{45}$$

$$M^* = \tilde{B} \left(\frac{1}{R^*} - \epsilon^2 R^* \frac{d\hat{\phi}}{d\sigma} \right), \tag{46}$$

$$\hat{\phi} = R^* \frac{dR^*}{d\sigma}, \tag{47}$$

$$\alpha \frac{d}{d\sigma} \left(R^{*5} \frac{dP^*}{d\sigma} \right) + \left(P^*_{\text{ext}} + \tilde{\Pi} - P^* \right) = 0; \tag{48}$$

where $\tilde{B}$, α and $\tilde{\Pi}$ are dimensionless constants given by

$$\tilde{B} = \frac{B}{\bar{r}^3 (p_e - p_b)}, \qquad \alpha = \frac{\bar{r}^3}{16 \mu \kappa L^2}, \qquad \tilde{\Pi} = \frac{\Pi}{p_e - p_b}.$$

Henceforth we will omit the stars from the dimensionless parameters.

We now consider the distinguished limit where $\tilde{B} = O(1)$ (justified in Section 2.3). We expand in powers of ϵ as follows[1]:

$$T = T_0 + \epsilon T_1 + \ldots, \qquad Q = Q_0 + \epsilon Q_1 + \ldots, \qquad M = M_0 + \epsilon M_1 + \ldots,$$
$$\hat{\phi} = \hat{\phi}_0 + \epsilon \hat{\phi}_1 + \ldots, \qquad R = R_0 + \epsilon R_1 + \ldots, \qquad P = P_0 + \epsilon P_1 + \ldots.$$

We know that the leading order terms of R and $\hat{\phi}$ are order 1 terms because of the self-evidently appropriate scalings that were used. However, it is not immediately clear that the same will be the case for T, Q and M. Despite this potential problem, substituting M and R into equation (46) and considering only the highest order terms yields the result that to leading order M is given by

$$M_0 = \frac{\tilde{B}}{R_0}.$$

[1]To be completely correct, we expect that the leading order terms of T and P will be $O(\max(1, \tilde{\Pi}))$, rather than $O(1)$. Fortunately, this does not change the following analysis. It should be noted, however, that for T and P the notation of a subscript 0 refers to the fact that the terms are leading order, *not* the fact that they are $O(1)$.

However, when this is substituted into equation (45), this leads to the result that the leading order term of Q is $O(\epsilon)$; that is, $Q_0 = 0$ and

$$Q_1 = \frac{\tilde{B}\hat{\phi}_0}{R_0^2}.$$

We now substitute this result for Q into equations (43) and (44)and find that the dominant balance in equations (43) and (44) will not include Q at all. This means that we may decouple Q and M from our system and consider only T, R, $\hat{\phi}$ and P. Indeed, it can be shown that as long as $\tilde{B} = o\left(\frac{1}{\epsilon^2}\right)$, Q will be sufficiently small for M and Q to be negligible when trying to solve for the other parameters.

Considering the leading order terms of equation (43), (44) and (47), we obtain the following system:

$$R_0\frac{d}{d\sigma}(R_0T_0) - \hat{\phi}T_0 = \frac{R_0^2}{2}\,\frac{dP}{d\sigma}, \tag{49}$$

$$T_0 = R_0(P_0 - P_{\text{ext}}), \tag{50}$$

$$\hat{\phi}_0 = R_0\frac{dR_0}{d\sigma}. \tag{51}$$

Henceforth, we will always be referring to the leading order given above, so we will omit the subscripted zeros.

Substituting equation (51) into (49) and simplifying, we find that

$$\frac{dT}{d\sigma} = \frac{R}{2}\,\frac{dP}{d\sigma}.$$

Now, substituting equation (50) into this expression yields

$$\frac{d}{d\sigma}(R(P - P_{\text{ext}})) = \frac{R}{2}\,\frac{dP}{d\sigma}.$$

We have simplified our system to the point where we have a two equations in two unknowns (R and P) that should capture all of the relevant behaviour of our axon. The leading order of our nondimensionalised system yields the following pair of differential equations:

$$\alpha\frac{d}{d\sigma}\left(R^5\frac{dP}{d\sigma}\right) + \left(P_{\text{ext}} + \tilde{\Pi} - P\right) = 0,$$

$$\frac{d}{d\sigma}(R(P - P_{\text{ext}})) = \frac{R}{2}\,\frac{dP}{d\sigma}.$$

Appendix D

List of participants in group

- Leah Band
- Mark Blyth
- Alex Foss (presenter)
- Claire Grills
- Cameron Hall
- Oliver Jensen
- Matthew Johnston
- John King
- Jonathon Moles
- Shailesh Naire
- Colin Please
- Giles Richardson
- Jennifer Siggers